Nanoscale Features of Fibronectin Fibrillogenesis Depend on Protein-Substrate Interaction and Cytoskeleton Structure

Tilo Pompe, Lars Renner, and Carsten Werner
Institute of Polymer Research Dresden and Max Bergmann Center of Biomaterials Dresden, 01069 Dresden, Germany

ABSTRACT   Cell-reorganized fibronectin layers on polymer films providing a gradation of the binding strength between protein and substrate were analyzed by combined fluorescence and scanning force microscopy. The nanoscale fibronectin patterns exhibited paired parallel fibrils with characteristic spacings of 156, 233, 304, and 373 nm. These spacings depend on the interaction of fibronectin with the substrate: at enhanced fibronectin-substrate anchorage the cells form larger stress fibers, which are assembled by α-actinin cross-linked pairs of actin filaments subunits at the focal adhesions. A ubiquitous repeating unit of ~71 nm was found within these characteristic distances. We conclude that the dimensions of the actin stress fibers reflect the binding strength of fibronectin to the polymer substrate and act—in turn—as a template for the reorganization of fibronectin into surface-bound nanofibrils with characteristic spacings. This explanation was confirmed by data showing the α-actinin/fibronectin colocalization.

INTRODUCTION

Fibronectin fibrillogenesis, the process by which several cell types create and arrange parts of the extracellular matrix into fibrillar networks, is at present intensively investigated (Hynes, 1999; Vogel et al., 2001; Wierzbicka-Patynowski and Schwarzbauer, 2003). A wealth of details on the complex mechanism of the formation of fibronectin fibrils is already known. It is widely accepted that stretching the dimeric 440 kDa molecule fibronectin (FN) is necessary to expose cryptic binding sites, which are involved in the polymerization process of fibril formation (Zhong et al., 1998). These forces can be exerted by the cells from the actin cytoskeleton via binding of the integrins to FN (Baneyx et al., 2002), whereas specific integrins like $\alpha_5\beta_1$ play a predominant role, because of their high affinity to the RGD cell-binding domain on the 10th FN-III repeating unit (Pankov et al., 2000; Sottile et al., 2000; Pankov and Yamada, 2002). Furthermore, transport of $\alpha_5\beta_1$-integrins along the actin stress fibers was observed (Pankov and Yamada, 2002) and assumed to be the transport mechanism involved in the formation of elongated FN fibrils leading to similarities in pattern of cytoskeleton elements and FN fibrils (Hynes and Destree, 1978). Additionally, other FN domains like the heparin binding domain near the N-terminus have been shown to be crucial for FN fibrillogenesis (Christopher et al., 1997). To unravel the mechanism of cellular fibrillogenesis the formation of FN fibrils was studied in several artificial systems. Conformational changes of FN were induced chemically by different concentrations of guanidine or mechanically by spreading FN monolayers on a Langmuir

trough aiming toward a formation of FN fibrils (Chen et al., 1997; Baneyx and Vogel, 1999). Although fibrillogenesis could be induced, structural differences in the nanometer range were observed in comparison to the FN fibrils formed in vivo (Chen et al., 1997), demonstrating the importance of the active stretching process by the cells. Theoretical studies and scanning force spectroscopy revealed the range of forces necessary to unravel cryptic sites important for FN polymerization (Craig et al., 2001; Oberhauser et al., 2002). Recent studies further demonstrated the strong correlation of FN fibrillogenesis to the active stretching and transport of FN by analyzing substrate dependent variations in the reorganization of preadsorbed FN by adherent cells (Altankov et al., 1996; Pompe et al., 2003a).

Several recent investigations concluded that the physicochemical state of FN is determined by the kind and density of chemical functionalities exposed by the substrate (Katz et al., 2000; Keselowsky et al., 2003; Faucheux et al., 2004). Changes in conformation, binding of integrins, as well as availability for reorganization processes and formation of focal adhesions could be related to the presence of surface functionalities such as $-CH3$, $-NH2$, $-COOH$, and $-OH$ moieties or to the chemical reactivity of the surface toward proteins. Furthermore, the differentiation of osteoblasts (Garcia et al., 1999) and the angiogenesis of endothelial cells (Pompe et al., 2004) were shown to be directly related to the status of surface bound FN. In view of these findings the gradation of the binding state of FN to solid substrates could be expected to reveal details about the process of FN fibrillogenesis.

To address this task, this study combines the detailed analysis of FN nanopatterns with the defined gradation of the FN-substrate anchorage. The binding strength of FN toward the substrate was adjusted using a set of thin films of different alternating maleic anhydride copolymers containing

comonomers with varied alkyl chain length. Enhanced displacement of FN by other serum proteins and higher degrees of cellular FN reorganization were observed on the more hydrophilic substrates containing a higher mass fraction of maleic acid (Pompe et al., 2003a; Renner et al., 2004). As mechanical forces were convincingly shown to play a crucial role for FN fibrillogenesis the varied anchorage of FN to the substrates was expected to induce distinct structural features of the FN fibrils. The latter aspect was investigated by scanning force microscopy to reveal the nanometer structure of the surface-bound FN after cellular reorganization.

MATERIALS AND METHODS

Substrates and proteins

Poly(octadecene-*alt*-maleic anhydride) (POMA) (Polysciences, Warrington, PA), and poly(propene-*alt*-maleic anhydride) (PPMA) (special product of Leuna-Werke AG, Merseburg, Germany) films were produced by spin coating (RC5, Suess Microtec, Garching, Germany) of 0.08% and 0.1%, respectively, copolymer solutions in tetrahydrofuran or methylethylketone (Fluka, Deisenhofen, Germany) on top of coverslips (24 mm × 24 mm), which had been freshly oxidized in a mixture of aqueous solutions of ammonia (Acros Organics, Geel, Belgium) and hydrogen peroxide (Merck, Darmstadt, Germany) and thereafter surface-modified with 3-aminopropyl-dimethylethoxy-silane (ABCR, Karlsruhe, Germany). As thoroughly confirmed by previous own studies the applied spin-coating process reliably provides very smooth polymer films of a few nanometers in thickness. Further details of the preparation and characterization were published elsewhere (Pompe et al., 2003b). Autoclaving induced hydrolysis of the anhydride moieties to provide a surface exclusively bearing carboxylic acid groups, which are fully dissociated at the pH of the cell culture medium (Osaki and Werner, 2003). The surfaces of the different copolymers exhibited a different surface energy depending on the kind of the comonomer due to the different mass fraction of the maleic acid groups. It was characterized by a quasi-static advancing water contact angle (sessile drop method, G40, Kruess, Hamburg, Germany) of 100° and 38° (±3°) for POMA and PPMA, respectively. Before cell culture experiments the coverslips were coated with FN from human plasma (Roche, Basel, Switzerland) or fluorescent labeled FN (FN-TRITC) out of a solution of 50 μg/ml in PBS (Biochrom, Berlin, Germany) for 1 h. FN labeling was performed using the FluoReporter Tetramethylrhodamine Protein Labeling Kit (Molecular Probes, Eugene, OR).

The amount of preadsorbed FN was quantified by HPLC-based amino acid analysis as described in detail elsewhere (Salchert et al., 2003). Briefly, after acidic vapor phase hydrolysis, amino acids were fluorescence-labeled, separated with a HPLC system, and quantified by a fluorescence detector (Series 1100, Agilent Technologies, Böblingen, Germany).

The adsorption strength of FN was analyzed by protein exchange reactions over time periods of 48 h. Homo- and heterodisplacement by FN and human serum albumin were studied by quantification of the exchanged amount of fluorescent labeled FN by confocal laser scanning microscopy and of nonlabeled FN by HPLC analysis. Further details of this study are published elsewhere (Renner et al., 2004).

Cell culture and sample fixation

Human endothelial cells from the umbilical cord vein were collected and cultured in endothelial cell growth medium ECGM (Promocell, Heidelberg, Germany) with 2% fetal calf serum as described elsewhere (Pompe et al., 2003a). After FN or FN-TRITC coating of the coverslips and subsequent rinsing with PBS and preincubation with cell medium for 10 min to block unspecific substrate interactions, 3×10^4 cells were seeded on the coverslips. According to a protocol introduced by Garcia et al. (1999) the cells were fixed with 1 mM cell-impermeable sulfo-BSOCOES cross-linker (Pierce, Rockford, IL) for 15 min at 4°C after 50 min of cell culture. Subsequently, the cross-linker were quenched with 50mM Tris buffer and noncross-linked cell compartments were extracted in 0.1% SDS for 15 min with an additional washing in 0.1% SDS for 10 min. The coverslips were washed in PBS again and left in fresh PBS for microscopy analysis. This fixation technique cross-links the extracellular matrix without cross-linking intracellular compartments, which permits to subsequently extract the noncross-linked parts of the cell leaving behind the matrix structures. In control experiments with unlabeled FN fixed samples were stained with rabbit polyclonal antibodies to human FN (Rockland, Gilbertsville, PA) and secondary TRITC conjugated antibody donkey anti-rabbit IgG (Jackson ImmunoResearch, West Grove, PA). As this fixation and staining procedure provided similar results of FN fibril patterns as observed after standard paraformaldehyde fixation, the sulfo-BSOCOES fixation was concluded to largely maintain the FN conformation.

Immunofluorescence

After cell culture α-actinin was stained by mouse monoclonal antibody (Cymbus Biotechnology, Chandlers Ford, Great Britain) with fixation of the cells in methanol at −20°C for 5 min and subsequent washing in PBS for 30 min. Secondary antibody staining was performed with Alexa Fluor 488 goat anti-mouse IgG (Molecular Probes). Methanol fixation was used because it resulted in a much better signal-to-noise ratio for the α-actinin staining compared to standard paraformaldehyde fixation. Because the resulting α-actinin pattern very well depicts the overall cytoskeletal structure—as it could be reasonably expected for a cross-linking element—the fixation technique was concluded to produce qualitatively and quantitatively reliable results.

Microscopy

Reorganized FN fibrils were analyzed after fixation and cell extraction with a scanning force microscope (SFM) (Bioscope, Veeco Instruments, Mannheim, Germany) equipped with a Q-Control device (nanoAnalytics, Münster, Germany) in TappingMode in PBS. The SFM was coupled to a confocal laser scanning microscope (TCS SP, Leica, Bensheim, Germany) to visualize FN-TRITC labeled FN fibrils during SFM imaging. The laser scanning microscope was equipped with a 40× immersion oil objective.

Image analysis

SFM images were analyzed by the Nanoscope software (Veeco Instruments) to measure the spacings between FN fibrils. The spacings of all paired nanofibrils were measured perpendicular to the fibril orientation in height images taken at different magnifications. Images of two or three arbitrarily chosen cells in five independent experiments were analyzed.

Immunofluorescence images were analyzed with Openlab software (Improvision, Coventry, Great Britain). α-actinin staining intensity was determined by localizing objects of FN-TRITC and α-actinin in the appropriate images, calculating the overlap (colocalization) of the objects areas of both images, and measuring α-actinin intensity in these colocalized regions. Data analysis including curve fitting were performed with ORIGIN (OriginLab, Northampton, MA) software.

Statistical analysis

Unpaired *t*-test analysis was performed for the evaluation of the intensity of α-actinin clusters.

RESULTS

FN fibrillogenesis was investigated in dependence on the bond strength of FN to different copolymer substrates. Details of FN adsorption and displacement at the same set of polymer substrates were analyzed in earlier studies (Pompe et al., 2003a; Renner et al., 2004). Briefly, the amount of adsorbed FN out of solutions of 50 μg/ml after 1 h was determined with 510 ± 20 ng/cm^2 and 470 ± 70 ng/cm^2 for POMA and PPMA, respectively, by HPLC analysis. Whereas the adsorbed amount was rather similar on the compared polymer surfaces, the bond strength of FN to the substrates was verified by protein displacement experiments with human serum albumin to be different, as illustrated in Fig. 1. Therein, the time-dependent FN-TRITC surface concentration is shown over a time period of 48 h in a solution of 50 μg/ml of human serum albumin measured by confocal laser scanning microscopy. A clear substrate dependence of the FN displacement is observed, indicating a less efficient protein exchange due to the higher interaction strength of FN with the substrate on the more hydrophobic POMA surface. Hence, a well-defined variation of the physicochemical surface characteristics is achieved in respect to the number of carboxylic acid groups at the copolymer surface. This change in the number of polar groups on the surface was verified by the change in hydrophobicity (water contact angle), XPS analysis, and electrokinetic measurement in earlier studies (Osaki and Werner, 2003; Pompe et al., 2003b). By that it was concluded that the used maleic anhydride copolymer thin films allow for a substrate-protein interaction in a controlled manner.

Based on these experiments, cell culture studies using this set of substrates revealed significant differences in the degree of reorganization of preadsorbed FN in the early stages of endothelial cell adhesion (50 min after seeding) depending on the FN-substrate a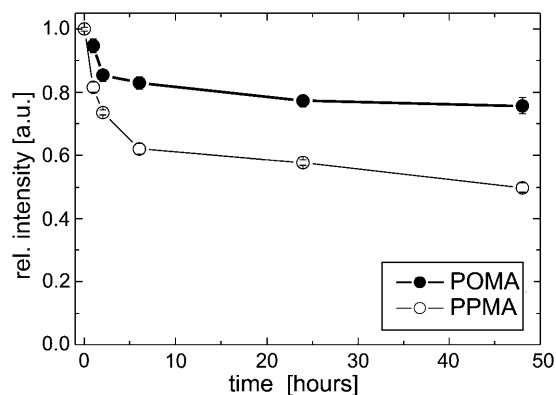nchorage (Pompe et al., 2003a) as well as a gradation in the cell-matrix reorganization at longer culture periods (Pompe et al., 2004). Starting from these findings obtained by fluorescence microscopy, the experiments performed in the current investigation determined the nanoscale characteristic of FN fibrils by SFM on similar FN-precoated PPMA and POMA thin films at 50 min after seeding of endothelial cells. The well-spread and adherent cells were fixed by cross-linking on the extracellular side, i.e., by using a water-soluble cross-linker, followed by the extraction of the nonfixed intracellular compartments, according to the technique introduced by Garcia et al. (1999). Due to those fixation and extraction procedures it is possible to image the reorganization patterns beneath the cells by SFM. The SFM analysis under PBS buffer conditions provides the possibility of a nanoscale investigation of the extracellular protein structures on the substrate surface at almost physiological conditions. By direct combination of fluorescence confocal laser scanning microscopy and SFM—on the same microscope stage—the analyzed protein structures could be confirmed to be extracellular FN assemblies. Fig. 2 *A* provides an exemplary fluorescence confocal laser scanning microscopy image of reorganized FN-TRITC fibrils on a PPMA substrate after 50 min of cell-substrate interaction. It clearly shows typical FN fibrils reorganized by endothelial cells. The corresponding SFM image of the same sample area is provided in Fig. 2 *B*. It demonstrates the coincidence of the visualized structures. In control experiments with unlabeled FN it was further verified that the FN fibril formation was unaffected by the TRITC conjugation of FN. Subsequent fluorescence staining with polyclonal antibodies to human FN revealed similar patterns as observed with directly labeled FN. The investigations were limited to a time course of 50 min to minimize the synthesis and secretion of FN by the cells and to restrict the FN fibrillogenesis to preadsorbed FN on the copolymer substrates. Suppressing protein synthesis by serum free cell culture conditions or by cyclohexinimide was not used herein to exclude possible influences of these artificial conditions on the FN fibrillogenesis by the cells.

The nanometer resolution of SFM provided the possibility to analyze structural details of FN fibrils. As summarized in a previous article (Pompe et al., 2003b), SFM analysis of the plain polymer-coated substrates could convincingly demonstrate the very smooth and homogeneous characteristics of the surfaces with a negligible roughness below 1 nm. Fig. 3 shows a typical high resolution image of FN fibrils on both substrates. The nanostructure reveals paired smaller fibrils that appear in optical microscopy as a single fibril. Section cuts along the white lines drawn in Fig. 3, *A* and *B*, are shown in Fig. 4, *A* and *B*, respectively, demonstrating typical heights of the FN fibrils in the range of 7 nm to 30 nm. As FN reorganization was previously shown to be different on the hydrophobic POMA substrates (Pompe et al., 2003a), the nanoscale analysis of the fibrils on POMA shows differences in comparison to the hydrophilic PPMA substrate, too (see

FIGURE 1 Dynamic displacement characteristic of FN-TRITC on POMA and PPMA in a solution of 50 μg/ml of human serum albumin over 48 h measured by confocal laser scanning microscopy. The error bars indicate the mean error from three independent experiments with each having 10 measurements per data point.
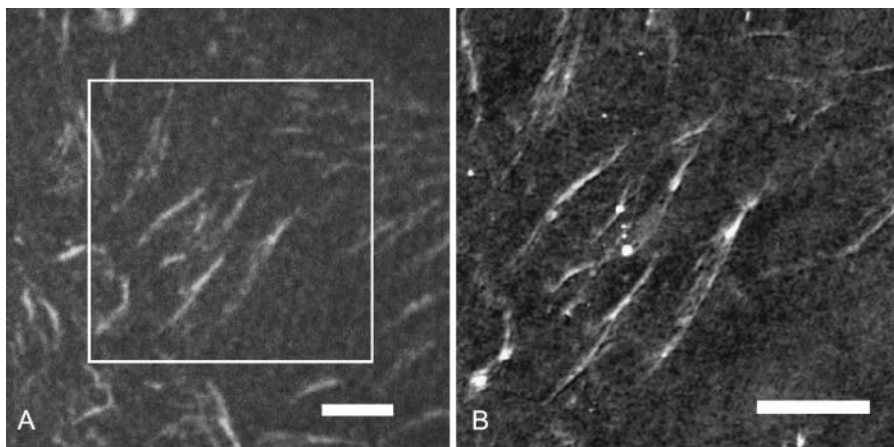
FIGURE 2 Analysis of TRITC conjugated FN fibrils on PPMA after reorganization by endothelial cells using a coupled fluorescence confocal laser scanning microscopy and SFM. (A) Optical image. Scale bar, 5 μm (B) SFM image of one part of image in Fig. 2 A. The cutout is marked in Fig. 2 A by a square. Scale bar, 5 μm (height scale, 50 nm).

Fig. 3 B). Although paired nanofibrils can also be observed on this substrate the general pattern appears to be different: the fibrils are often shorter and thicker, although the spacing between the nanofibrils is larger. The comparison of the section cuts of the FN fibrils along the white lines drawn in the topographical images of Fig. 3, A and B, underlines these observations (see Fig. 4, A and B) with an increased spacing of nanofibrils on the POMA substrate.

A statistical analysis of all spacings of paired nanofibrils perpendicular to the fibril orientation (as indicated in Fig. 4) in the recorded SFM images of different magnification revealed the occurrence of characteristic numbers. In five independent experiments the reorganized fibril pattern of two or three arbitrary chosen cells were analyzed from the height images. A histogram of the analysis with 45 measurements for each substrate is plotted in Fig. 5. The two different substrate characteristics result in clearly distinguished magnitudes of the typical spacing between the reorganized nanofibrils. By fitting a Gaussian function into four major peaks of the measured values 156 nm and 233 nm for PPMA and 304 nm and 373 nm for POMA were determined as the

typical spacings. The nearly similar difference between these values strongly suggests a fundamental structuring element (repeating unit) involved in the process of fibrillogenesis.

By fitting a periodic squared sine function to the four major peaks of the measured spacings, the repeating unit was estimated to 71 nm as shown in Fig. 6. Interestingly, this value equals twice the smallest measured spacing. Referring to the current model on FN reorganization this periodicity can be assumed to be originated by intracellular cytoskeletal elements, because the cytoskeleton acts on the FN molecules via integrins. Out of the variety of cytoskeleton-associated molecules α-actinin was found as a candidate component to cause the observed periodicity (Tsuruta et al., 2002; von Wichert et al., 2003): actin filaments cross-linked by α-actinin exhibit a typical spacing in the range of 34–39 nm, which is half the length of the observed value (Meyer and Aebi, 1990; Taylor et al., 2000).

To verify this hypothesis the α-actinin concentration colocalized or associated with FN fibrils was determined by immunofluorescence staining and fluorescence microscopy. An increase in fluorescence intensity for nanofibrils with
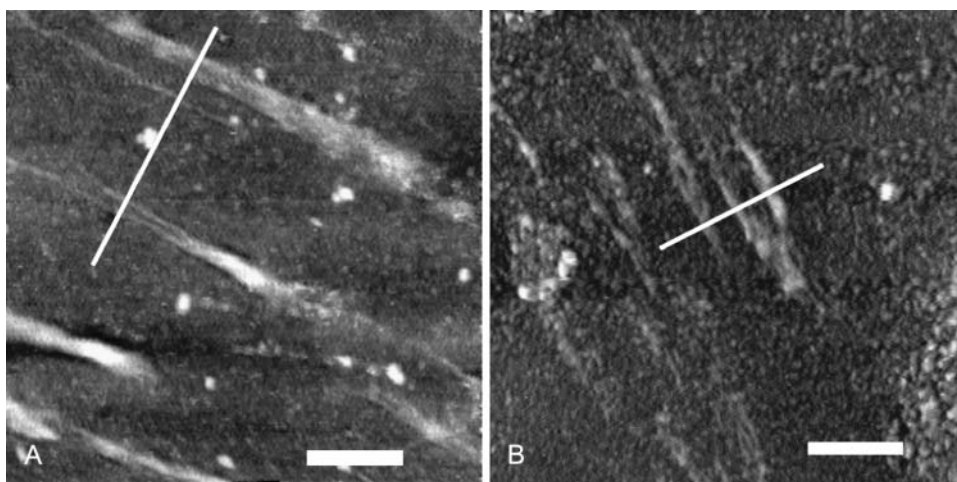

FIGURE 3 SFM height images of FN fibrils on PPMA (A) and POMA (B). The white lines indicate section cuts shown in Fig. 5. Scale bars, 1 μm. Height scale, 70 nm.
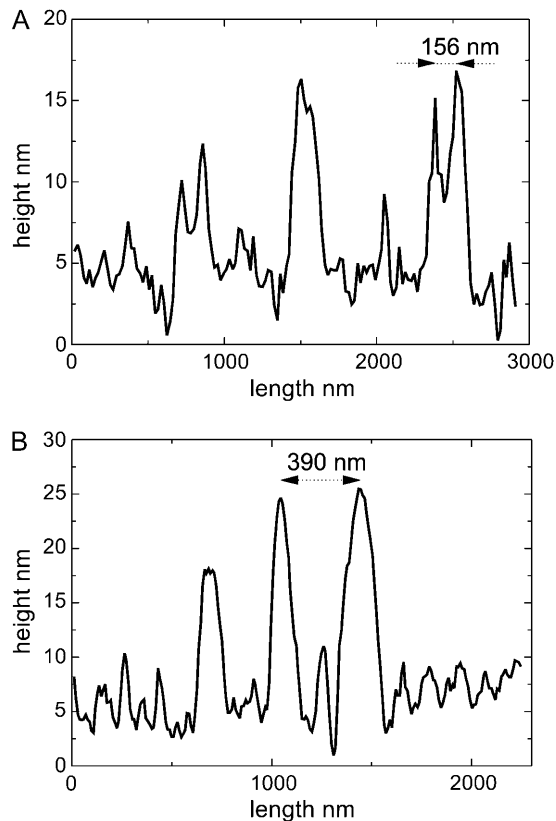
FIGURE 4 Graphs of line sections of the SFM topography images in Fig. 3, *A* (PPMA) and *B* (POMA), indicating the height of the FN fibrils and the spacing between them.

larger spacings can be expected since fluorescence microscopy can only reveal a summed signal of the nanometer separated α-actinin structures. With the resolution limit of ~300-nm signals from smaller structures—such as the hypothesized α-actinin cross-linked actin stress fibers between the FN nanofibrils—will be summed into one α-actinin concentration dependent signal.
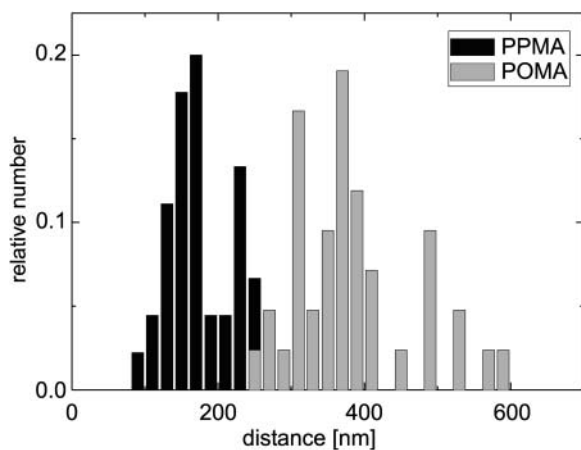

FIGURE 5 Histogram of typical spacings of paired FN nanofibrils on the two different substrates with 45 measurements for each substrate.
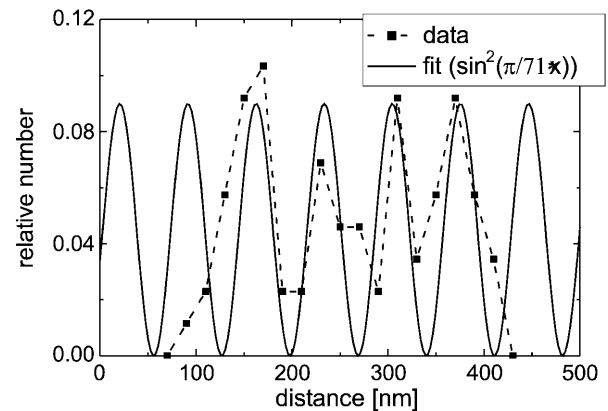

FIGURE 6 Fitting a periodic squared sine function to the histogram data of both substrates of Fig. 6. A repeating unit of 71 nm could be determined.

Fig. 7 illustrates the typical images analyzed from two independent cell experiments of α-actinin clusters stained with Alexa Fluor 488 conjugated antibodies next to fibrils of FN-TRITC. A higher intensity of α-actinin is observed on the hydrophobic POMA substrate (Fig. 7 *A*) where FN was more tightly immobilized than on the more hydrophilic PPMA substrate (Fig. 7 *B*). Fig. 8 shows the quantitative analysis of the mean fluorescence intensities of α-actinin clusters colocalized or associated with FN fibrils from one typical experiment with an automatic analysis of 60 colocalized clusters and 7 associated clusters chosen directly by eye. Associated clusters are meant to be clusters of partly overlapping FN fibrils in the direction of their growth (toward the center of the cell contour). A higher intensity is observed for α-actinin clusters in cells on POMA surfaces. A comparison of the ratio of the mean α-actinin intensities on both surfaces (PPMA and POMA) with the ratio of the mean observed FN nanofibril spacing revealed a very good agreement as presented in Fig. 8 *B*. The rather large error range is mainly caused by the error propagation when calculating the intensity and spacing ratios for the two substrates.

DISCUSSION

The SFM nanoscale analysis of FN fibrils reorganized by endothelial cells on polymer substrates with different bond strength to immobilized FN provided new insights in the process of FN fibrillogenesis. The defined gradation of the physicochemical surface characteristics of the polymer substrates allowed for a distinct control of the FN-substrate interaction. The varying density of maleic acid groups at the different substrate surfaces, verified by contact angle goniometry, XPS analysis, and electrokinetic measurements in earlier studies (Osaki and Werner, 2003; Pompe et al., 2003b), are accounted for the change in FN-substrate bond strength, which was demonstrated in the varying FN exchange characteristics by human serum albumin (Renner et al., 2004). Whereas earlier studies based on fluorescence
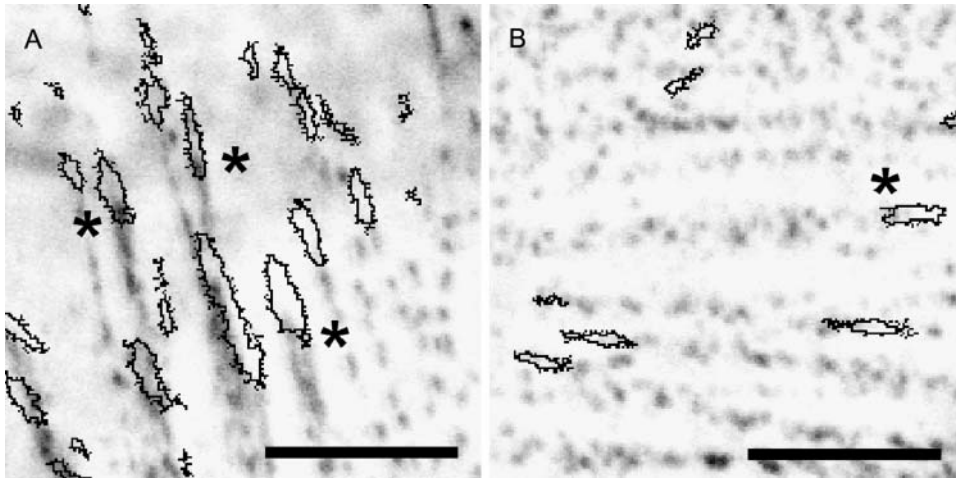
FIGURE 7 α-Actinin staining of endothelial cells after 50 min of reorganization of preadsorbed TRITC conjugated FN on the two copolymer substrates (*A*, POMA; *B*, PPMA). Contours of FN fibrils are drawn over the α-actinin fluorescence intensity image. The asterisks indicate pronounced colocalization or association of FN fibrils and α-actinin clusters. Scale bar, 5 μm.

microscopy further demonstrated that such differences in the FN-substrate anchorage could switch the degree of FN-reorganization by adherent endothelial cells (Pompe et al. 2003a, 2004), the current SFM-based work could substantially extend this investigation by revealing for the first time distinct differences in the nanoscale pattern of the extracellular FN fibril assembly in PBS buffer environments.

FN nanofibrils were observed and distinguished with respect to their structural characteristics. Fluorescence labeling allowed us to identify the FN fibrils by laser scanning microscopy whereas detailed analysis with nanometer resolution was achieved by the coupled scanning force microscope. The height range of 7 nm to 30 nm observed for the substrate-bound FN nanofibrils agrees well with previous reports in the literature (Chen et al., 1997; Hynes, 1999). The

FIGURE 8 (*A*) α-Actinin concentration determined by antibody staining intensity measured with confocal laser scanning microscopy. The mean intensity of α-actinin was measured at areas colocalized with FN fibrils (60 clusters) and at areas of α-actinin clusters partly colocalized (associated) with FN fibrils (seven clusters). The mean intensities for the two substrates are statistically different on a significance level of $p < 10^{-5}$. (*B*) Ratio of mean α-actinin concentration colocalized or associated with FN fibrils compared with ratio of mean FN nanofibril spacing on the two different copolymer substrates. Error bars indicate the calculated propagated error of all measurements.

quantified spacings of the nanofibrils were found to be larger on the hydrophobic POMA, where FN has been demonstrated to be more tightly bound than on the less hydrophobic PPMA (Renner et al., 2004). The different hydrophobicity of the used substrates originates from the variable surface density of polar maleic acid groups as described elsewhere (Osaki and Werner, 2003; Pompe et al., 2003b). It is known that FN fibrillogenesis occurs as the consequence of tensile forces exerted by the cells via the cytoskeleton, which stretch FN molecules to expose cryptic binding sites for the FN polymerization (Hynes, 1999; Vogel et al., 2001; Wierzbicka-Patynowski and Schwarzbauer, 2003). Hence, it is reasonable to assume that larger forces are required to stretch and transport the FN on substrates where the protein is immobilized with higher bond strength. Furthermore, it is known that the cells can regulate by integrin binding the focal adhesion size and the strength of tensile forces acting by the actin cytoskeleton in dependence on the bond strength of the extracellular matrix proteins to the substrate (Balaban et al., 2001; Galbraith et al., 2002; Pankov et al., 2002). In this context the FN fibril structures on the substrates used in this study first of all confirm that anchorage of the protein to the substrate is reflected by the fibril pattern with larger spacings on the substrate with stronger FN anchorage.

The fact that spacings of FN nanofibrils were detected to be multiples of 71 nm suggests a close interrelation of the FN fibrillogenesis with nanoscale intracellular structures. The spacing of 71 nm would coincide with twice the spacing of α-actinin cross-linked actin filaments, which was found to be 34–39 nm (Meyer and Aebi, 1990; Taylor et al., 2000). After this coincidence, the formation of FN fibrils by the transport of integrin-bound FN along actin stress fibers (Pankov and Yamada, 2002) could cause spacings of the formed FN nanofibrils according to the size of the actin stress fibers. Interestingly, the FN fibril spacing was found to be restricted to discrete spacings corresponding to odd numbers of actin filaments cross-linked by α-actinin. The odd numbers of actin filaments and the occurrence of twice the α-actinin
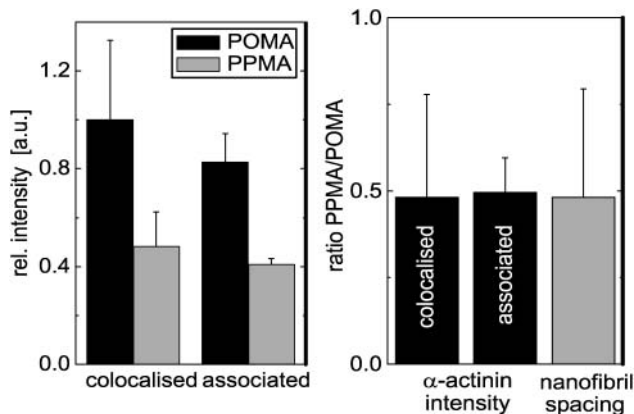
length can be attributed to the inner structure of actin stress fibers with anti-parallel orientation of actin filaments (Alberts et al., 1994). It has to be mentioned that parallel and anti-parallel orientations of actin filaments were observed depending on cell type, kind of actin bundles, and cross-linking protein (Meyer and Aebi, 1990; Cramer et al., 1997). However, the basic mechanism of the myosin-driven stress exertion in the stress fibers due to the movement of the myosin motors toward the plus end of the actin filament would suggest the existence of an anti-parallel actin filament orientation in agreement with the observed repeating unit of twice the α-actinin length. As the FN transport along the stress fibers together with the integrin linker is myosin-driven, too, the occurrence of a repeating unit of twice the α-actinin length can be related to the inner actin stress fiber structure. This hypothesis suggesting a key role of α-actinin and the actin filament structures for the FN fibrillogenesis was further supported by the concentration of these cytoskeletal elements at the location of the FN fibril formation shown in Fig. 8. The data display higher α-actinin concentrations at higher FN nanofibril spacings on POMA where FN reorganization was found to be hampered by stronger binding between the protein and the substrate when compared to FN on PPMA. This confirms the relation of the reported findings to the action of the cytoskeletal force transduction apparatus, which is sensitive to the anchorage of the extracellular matrix proteins to the underlying substrate. Since the direct correlation of FN fibrils with actin stress fibers is well known (Hynes, 1999), the actin cytoskeleton was not investigated in this study. Instead, emphasis was set on α-actinin, which is considered to be the structural element creating the observed FN fibril spacings. Also, the size of the focal adhesions can be expected to display the force related to the FN-substrate anchorage (Balaban et al., 2001). This was investigated for the analyzed set of systems in a companion study that will be reported elsewhere (T. Pompe, unpublished data).

The occurrence of FN fibril spacings with a repeating unit related to the α-actinin governed actin filament spacings is

further supported by the recently observed feature of a square lattice for the inner structure of actin stress fibers (Pelletier et al., 2003). Such a square lattice would allow for the exact periodic reproduction of the spacing of α-actinin cross-linked filaments to the outside of a bigger actin stress fiber, which can function as a template for FN fibril formation. Any other packing of actin filaments in a stress fiber like a hexagonal lattice packing would contradict the observed regular spacing because the resulting stress fiber would exhibit a more cylindrical overall shape and could not regenerate templates resulting in all the observed spacings of 156, 233, 304, and 373 nm corresponding to 5, 7, 9, and 11 α-actinin cross-linked actin filaments. The minimal possible spacing of 71 nm was not observed, which would suggests, that the weakest FN bond strength obtained in our experiments for the PPMA substrate is still high enough to enable the assembly of actin stress fibers exceeding the minimum size.

Out of the presented data, a mechanism (illustrated in Fig. 9) is suggested that relates FN fibrillogenesis to the cellular feedback cycle at the focal adhesions: the bond strength of immobilized FN is sensed by the cell via the integrins, other proteins at the focal adhesion and the actin cytoskeleton. Accordingly, the cell assembles actin stress fibers triggered by the Rho pathway to exert a force adequate to the bond strength of the immobilized FN (Balaban et al., 2001; Zamir and Geiger, 2001), which should manifest itself in the size of the focal adhesions/integrin clusters, too. Along the α-actinin cross-linked actin stress fibers structurally related FN fibrils are formed by stretch, transport, and subsequent polymerization of FN. The inner square lattice structure of the actin stress fibers determine the dimensions of the FN fibrils causing a discrete spacing related to the spacing of pairs of α-actinin cross-linked actin filaments. In consequence, a higher bond strength of FN to the substrate—i.e., to POMA substrates in comparison to PPMA substrates—results in thicker α-actinin cross-linked actin fibers and larger spacings of the FN nanofibrils. The occurrence of twice the α-actinin length as the repeating unit originates from the anti-parallel orientation of the actin filaments inside the actin stress fibers
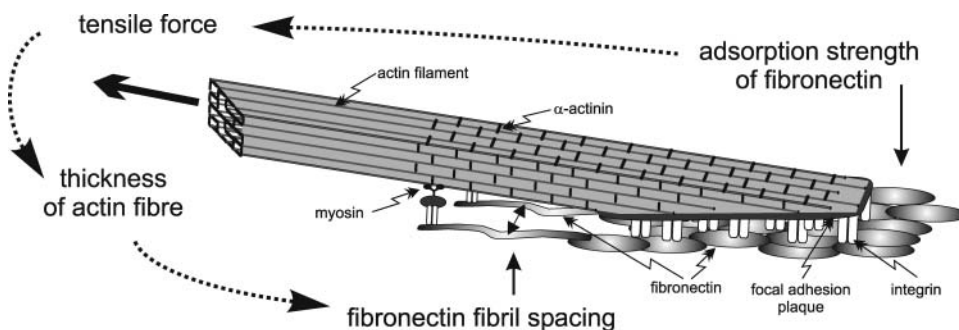

FIGURE 9 Schematic representation of the proposed model for the FN fibrillogenesis explaining the typical spacing of FN nanofibrils and its substrate dependence. Related to the gradated bond strength of FN to the substrate, the tensile force of the cell is adjusted, which acts in the actin stress fibers onto the substrate-bound FN molecules. In this process, the focal adhesion size and the thickness of actin stress fibers is regulated. This provides a distinct thickness of the actin stress fibers due to the α-actinin as the actin cross-linking element, which provides a pattern template for the FN fibril formation along the fibers by the myosin-driven FN stretching and transport. The discrete size of the actin stress fibers depends on their inner structure with a square lattice of α-actinin cross-linked actin filaments. Note that the sketch just illustrates the correlation of FN bond strength, stress fiber size, its inner structure, and fibronectin fibril spacing. Details of protein assembly and the structure of the focal adhesions are not in the scope of the figure.

and the myosin-driven transport and stress evolvement toward the plus ends of the actin filaments.

Altogether, the results of this work confirm the importance of force-structure relations in the process of FN fibrillogenesis. We suggest a new hypothesis explaining the role of molecular elements of the cytoskeleton and their interplay with environmental factors to determine the nanoscale patterns of FN fibrils. In turn, the presented data demonstrate the key role of the physicochemical characteristics of artificial surfaces to modulate cell-matrix adhesion via control over FN anchorage.

REFERENCES

Alberts, B., D. Bray, J. Lewis, M. Raff, K. Roberts, and J. D. Watson. 1994. Molecular Biology of the Cell, 3rd ed. Garland Publishing, New York.

Altankov, G., F. Grinnell, and T. Groth. 1996. Studies on the biocompatibility of materials: fibroblast reorganization of substratum-bound fibronectin on surfaces varying in wettability. *J. Biomed. Mater. Res.* 30:385–391.

Balaban, N. Q., U. S. Schwarz, D. Riveline, P. Goichberg, G. Tzur, I. Sabanay, D. Mahalu, S. Safran, A. Bershadsky, L. Addadi, and B. Geiger. 2001. Force and focal adhesion assembly: a close relationship studied using elastic micropatterned substrates. *Nat. Cell Biol.* 3:466–473.

Baneyx, G., L. Baugh, and V. Vogel. 2002. Fibronectin extension and unfolding within cell matrix fibrils controlled by cytoskeletal tension. *Proc. Natl. Acad. Sci. USA.* 16:5139–5143.

Baneyx, G., and V. Vogel. 1999. Self-assembly of fibronectin into fibrillar networks underneath dipalmitoyl phosphatidylcholine monolayers: role of lipid matrix and tensile forces. *Proc. Natl. Acad. Sci. USA.* 96:12518–12523.

Chen, Y., L. Zardi, and D. M. P. Peters. 1997. High-resolution cryo-scanning electron microscopy study of the macromolecular structure of fibrils. *Scanning.* 19:349–355.

Christopher, R. A., A. P. Kowalczyk, and P. J. McKeown-Longo. 1997. Localization of fibronectin matrix assembly sites on fibroblasts and endothelial cells. *J. Cell Sci.* 110:569–581.

Craig, D., A. Krammer, K. Schulten, and V. Vogel. 2001. Comparison of the early stages of forced unfolding for fibronectin type III modules. *Proc. Natl. Acad. Sci. USA.* 98:5590–5595.

Cramer, L. P., M. Siebert, and T. J. Mitchison. 1997. Identification of novel graded polarity actin filament bundles in locomoting heart fibroblasts: implications for the generation of motile force. *J. Cell Biol.* 136:1287–1305.

Faucheux, N., R. Schweiss, K. Lützow, C. Werner, and T. Groth. 2004. Self-assembled monolayers with different terminating groups as model substrates for cell adhesion studies. *Biomaterials.* 25:2721–2730.

Galbraith, C. G., K. M. Yamada, and M. P. Sheetz. 2002. The relationship between force and focal complex development. *J. Cell Biol.* 159:695–705.

Garcia, A. J., D. V. Vega, and D. Boettiger. 1999. Modulation of cell proliferation and differentiation through substrate-dependent changes in fibronectin conformation. *Mol. Biol. Cell.* 10:785–798.

Hynes, R. O. 1999. The dynamic dialogue between cells and matrices: implications of fibronectin's elasticity. *Proc. Natl. Acad. Sci. USA.* 96:2588–2590.

Hynes, R. O., and A. T. Destree. 1978. Relationships between fibronectin (LETS protein) and actin. *Cell.* 15:875–886.

Katz, Z., E. Zamir, A. Bershadsky, Z. Kam, K. M. Yamada, and B. Geiger. 2000. Physical state of the extracellular matrix regulates the structure and molecular composition of cell-matrix adhesions. *Mol. Biol. Cell.* 11:1047–1060.

Keselowsky, B. G., D. M. Collard, and A. J. Garcia. 2003. Surface chemistry modulates fibronectin conformation and directs integrin binding and specificity to control cell adhesion. *J. Biomed. Mater. Res.* 66A:247–259.

Meyer, R. K., and U. Aebi. 1990. Bundling of actin filaments by α-actinin depends on its molecular length. *J. Cell Biol.* 110:2013–2024.

Oberhauser, A. F., C. B. Fernandez, M. C. Vazquez, and J. M. Fernandez. 2002. The mechanical hierarchies of fibronectin observed with single-molecule AFM. *J. Mol. Biol.* 319:433–447.

Osaki, T., and C. Werner. 2003. Ionization characteristics and structural transitions of alternating maleic acid copolymer films. *Langmuir.* 19:5787–5793.

Pankov, R., E. Cukierman, B. Z. Katz, K. Matsumoto, D. C. Lin, S. Lin, C. Hahn, and K. M. Yamada. 2000. Integrin dynamics and matrix assembly: tension-dependent translocation of $\alpha 5\beta 1$ integrins promotes early fibronectin fibrillgenesis. *J. Cell Biol.* 148:1075–1090.

Pankov, R., and K. M. Yamada. 2002. Fibronectin at a glance. *J. Cell Sci.* 115:3861–3863.

Pelletier, O., E. Pokidysheva, L. S. Hirst, N. Bouxsein, Y. Li, and C. R. Safinya. 2003. Structure of actin cross-linked with α-actinin: a network of bundles. *Phys. Rev. Lett.* 91:148102.

Pompe, T., F. Kobe, K. Salchert, B. Jørgensen, J. Oswald, and C. Werner. 2003a. Binding strength of fibronectin to polymer substrates controls the initial phase of endothelial cell adhesion. *J. Biomed. Mater. Res.* 67A:647–657.

Pompe, T., M. Markowski, and C. Werner. 2004. Modulated fibronectin anchorage at polymer substrates controls angiogenesis. *Tissue Eng.* 10:841–848.

Pompe, T., S. Zschoche, K. Salchert, N. Herold, M. F. Gouzy, C. Sperling, and C. Werner. 2003b. Maleic anhydride copolymers — a versatile platform for molecular biosurface engineering. *Biomacromolecules.* 4:1072–1079.

Renner, L., T. Pompe, K. Salchert, and C. Werner. 2004. Protein exchange on copolymer substrates with graded physicochemical characteristics. *Langmuir.* 20:2928–2933.

Salchert, K., T. Pompe, C. Sperling, and C. Werner. 2003. Quantitative analysis of immobilized proteins and protein mixtures by amino acid analysis. *J. Chromatogr. A.* 1005:113–122.

Sottile, J., D. C. Hocking, and K. J. Langenbach. 2000. Fibronectin polymerization stimulates cell growth by RGD-dependent and -independent mechanisms. *J. Cell Sci.* 113:4287–4299.

Taylor, K. A., D. W. Taylor, and F. Schachat. 2000. Isoforms of α-actinin from cardiac, smooth, and skeletal muscle form polar arrays of actin filaments. *J. Cell Biol.* 149:635–645.

Tsuruta, D., M. Gonzales, S. B. Hopkinson, C. Otey, S. Khuon, R. D. Goldman, and J. C. R. Jones. 2002. Microfilament-dependent movement of the b3 integrin subunit within focal contacts of endothelial cells. *FASEB J.* 16:866–868.

Vogel, V., W. E. Thomas, D. W. Craig, A. Krammer, and G. Baneyx. 2001. Structural insights into the mechanical regulation of molecular recognition sites. *Trends Biotechnol.* 19:416–423.

von Wichert, G., B. Haimovich, G. S. Feng, and M. P. Sheetz. 2003. Force-dependent integrin-cytoskeleton linkage formation requires downregulation of focal complex dynamics by Shp2. *EMBO J.* 22:5023–5035.

Wierzbicka-Patynowski, I., and J. E. Schwarzbauer. 2003. The ins and outs of fibronectin matrix assembly. *J. Cell Sci.* 116:3269–3276.

Zamir, E., and B. Geiger. 2001. Molecular complexity and dynamics of cell-matrix adhesions. *J. Cell Sci.* 114:3583–3590.

Zhong, C., M. Chrzanowska-Wodnicka, J. Brown, A. Shaub, A. M. Belkin, and K. Burridge. 1998. Rho-mediated contractility exposes a cryptic site in fibronectin and induces fibronectin matrix assembly. *J. Cell Biol.* 141:539–551.